Self-excited Wave Propagation in a Reflective Shuttling Detonation Combustor

Michael Ullman[1], Supraj Prakash[1], Deborah Jackson[2], Venkat Raman[1], Carson Slabaugh[2], and John Bennewitz[3]

[1]University of Michigan, Ann Arbor, MI, USA
[2]Purdue University, West Lafayette, IN, USA
[3]Air Force Research Laboratory, Edwards, CA, USA

1 Introduction

Detonation combustors, such as rotating detonation engines (RDEs), have gained attention in recent years for the higher thermal efficiencies they offer over conventional constant-pressure combustion systems [1]. However, the unsteady, three-dimensional nature of these systems makes them difficult to study both numerically and experimentally. In particular, the effects of inflow conditions, fuel-oxidizer mixing, and other boundary conditions are not well understood. Previous studies have used simplified systems, such as linearized model detonation engines (LMDEs), to remove the effects of curvature and study the interaction between injected reactant mixtures and propagating detonation waves [2, 3]. These linearized systems typically do not consider the generation or interaction of multiple detonation waves, both of which play a key role in practical RDE systems. In both numerical [4] and experimental [5, 6] RDE studies, weak counter-rotating waves emerging from the primary detonation wave system have been observed. The impact of these waves on the propagation and bifurcation of the strong detonations is unclear, and targeted investigations of these dynamics are required to yield practical insights.

To provide increased optical accessibility and better understand the unsteady flow phenomena within RDEs, a reflective shuttling detonation combustor (RSDC) is considered. Here, the annular combustion chamber of the RDE is "unwrapped" and has reflective walls on one or both ends of the combustor, resulting in an open-closed or closed-closed configuration. In this setup, detonation waves propagate in both directions, capturing the dynamics of counter-rotating wave modes typically observed in RDE geometries. In particular, Yamaguchi et al. tested a novel fan-shaped RSDC in which waves could propagate and reflect between the two end walls of the combustion chamber [7]. In this study, a single detonation wave was observed travelling back and forth across the chamber. In a second study [8], researchers tested an RSDC with a rectangular combustion chamber and two closed transverse walls. Here, four unique wave modes were identified, including single and double detonation modes, a single strong-single weak detonation mode, and a deflagration mode. The appearance of these modes was found to correlate with the mass flow rate and equivalence ratio of the non-premixed reactant inflow. Also, the observed wave speeds were between 30-40% lower than the Chapman–Jouguet (CJ) speed—a result attributed to incomplete mixing and interactions between counter-propagating waves. Taguchi et al. observed similar correlations in their experimental closed-closed RSDC, and also noted that the wave speeds and appearance of different wave modes were linked to the length of the combustion chamber [9].

Correspondence to: mullman@umich.edu

To examine how such wave modes may appear under the influence of different boundary conditions, the present study investigates a rectangular RSDC with an open-closed combustion chamber configuration. This design, developed by Schwinn et al. [10], allows for interactions between strong detonation waves and reflected acoustic waves, thereby making it more applicable to the wave and mixing dynamics observed in practical RDE systems. This setup was previously used to study the origins and frequencies of self-sustained chamber dynamics under different flow and boundary conditions [10]. The details of the RSDC, along with the numerical configuration, are outlined in Sec. 2. The mechanisms leading to the development and stabilization of detonation within the combustor are discussed in Sec. 3, followed by operational characteristics of the RSDC under two inflow conditions.

2 Flow Configuration and Numerical Methods

The RSDC geometry considered in this study is shown in Fig. 1. The oxidizer manifold has five inlets and a continuous slot into the combustion chamber. The two fuel manifolds each have three inlets and 53 cylindrical injectors feeding the chamber. The top and far sides of the chamber are open boundaries, while the near side is a closed wall. To help dissipate exiting waves, an progressively-coarsened exhaust region was added to the top and side of the chamber. This region, not shown in Fig. 1, was constructed such that its far-field boundaries would not artificially influence the flow within or near the chamber.

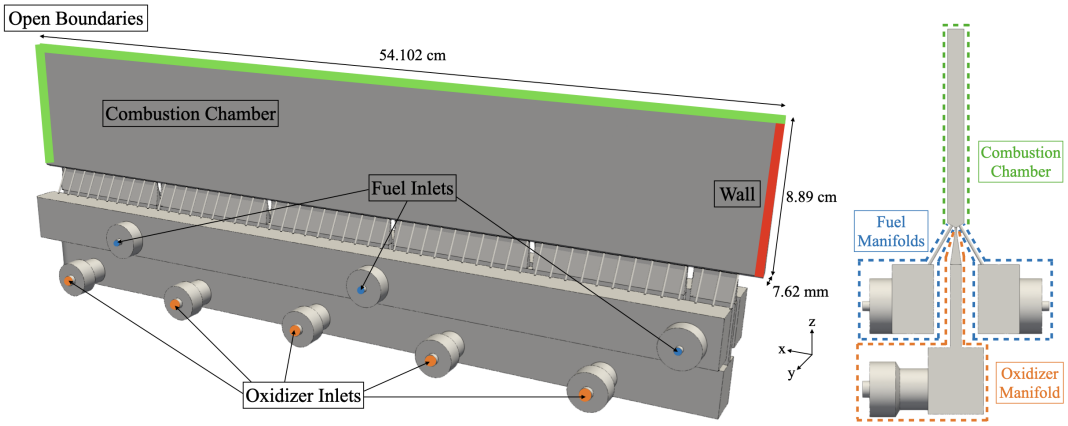

Figure 1: RDSC geometry, featuring one oxidizer manifold with five inlets and two fuel manifolds with three inlets each. Fuel enters the combustion chamber via 106 cylindrical injectors.

A high-fidelity simulation approach with no sub-grid scale turbulence models is used to study the detonation wave behavior within the open-closed domain configuration. The governing equations include mass, momentum, and energy conservation equations, along with species conservation equations to incorporate the chemical reactions. The in-house finite-volume compressible reacting flow solver UM-ReactingFlow is used to solve the Navier-Stokes equations using an ideal gas equation of state. Second-order MUSCL and second-order Runge-Kutta schemes are used for the spatial and temporal discretizations, respectively, and the HLLC approximate Riemann solver is used for convection. The diffusion terms are discretized using the second-order KNP method [11]. A 13-species, 38-reaction FFCMy-13 mechanism [12, 13] is used to model the chemical reactions. Computationally-intensive subroutines for convection and reaction stages are offloaded to the GPU using in-house CUDA-based modules for compatibility with heterogeneous computing platforms. For GPU-based reaction treatment, detailed chemical kinetics (chemical source term evaluation and stiff time integration) and thermodynamic gas properties are evaluated through a matrix-based formulation that maximizes throughput [14]. The solver

has been validated for various turbulent, reacting, and shock-containing flows [4, 15]. Using MPI-based domain decomposition, the solver is parallelized and executed on 6300 cores with 900 GPUs.

An unstructured mesh resolution of 200 μm was prescribed in the fuel injectors, oxidizer slot, and lower half of the combustion chamber. In the upper half of the chamber and regions just outside of its open boundaries, a resolution of 400 μm was prescribed. This resolution was chosen due to the broadened reaction zones and induction lengths expected in three-dimensional detonations with non-premixed inflows [2, 3]. This sizing allowed for at least 10 cells across the broadened induction length, and is similar to resolutions used in other three-dimensional detonation simulations [4,16]. Other studies have shown that further refinements did not significantly alter macroscopic quantities [17]. The chosen resolution in the injectors and chamber, along with further coarsening in the fuel and oxidizer manifolds and exhaust region, resulted in a total of 62.5 million control volumes.

The simulated flow conditions are given in Table 1. In each case, the fuel and oxidizer manifolds were initialized to their respective pressures and species concentrations at 300 K. Here, pure methane and diatomic oxygen are used as the fuel and oxidizer, respectively. The remainder of the domain was initialized with air at atmospheric conditions. The fuel and oxidizer inflows were prescribed choked mass-flow conditions, and the walls were given adiabatic, no-slip conditions. The far-field was given a subsonic outflow condition at atmospheric pressure. Non-reacting flow was allowed to develop for 0.5 ms, at which point a 3 cm $\times$ 1 cm linear detonation ramp profile was patched into the bottom of the combustion chamber near its closed end. The flow field was then allowed to develop for 5 ms after ignition, giving sufficient time to establish quasi-steady-state wave behavior within the chamber.

The simulations captured the wave behavior under two inflow conditions: lean (Case 176) and rich (Case 182). The results were compared to experiments conducted at Purdue University for similar lean (Case 207) and rich (Case 271) scenarios. In the experimental setup, the fuel was natural gas instead of pure methane. However, additional experiments with methane showed only a marginal difference in wave speed, frequency, and strength.

Table 1: Simulation and experiment test configurations.

Type	Case	Mass Flux [kg/s/m^2]	ϕ	Fuel Flow Rate [kg/s]	Oxi. Flow Rate [kg/s]	Fuel Mani. Pressure [MPa]	Oxi. Mani. Pressure [MPa]
Sim.	176	121	0.80	0.081	0.394	0.361	0.361
	182	120	1.15	0.108	0.364	0.453	0.326
Exp.	207	121	0.81	0.086	0.414	0.338	0.396
	271	119	1.20	0.116	0.373	0.455	0.377

3 Results and Discussion

Both simulated scenarios exhibit a similar progression toward self-excited steady-state wave behavior. First, the initial detonation wave traverses the chamber and exits the open end, creating choked flow at the top and side exit planes. This creates acoustic reflections into the chamber—particularly at the corner between the two open boundaries. These reflected waves travel back toward the closed end of the chamber, gradually transitioning to weakly reacting waves as they interact with fresh reactant gases. After reflecting off of the closed transverse wall, the waves transition to strong detonations which accelerate and expand as they traverse the length of the chamber. These waves create open boundary reflections akin to the initial acoustic wave, thereby facilitating a self-excited quasi-steady-state wave behavior characterized by weak left-running waves and strong right-running waves. Choking continues to occur at the exit planes of the chamber only during the passage of waves, as the mean

chamber pressure is below the critical pressure. Instantaneous pressure snapshots taken 4.2 ms after ignition along the mid-plane of the domain are shown in Fig. 2. These snapshots were taken during quasi-steady-state operation, which is illustrated in the detonation surface plots in Fig. 3. Here, weaker left-running waves collide with stronger right-running waves before reflecting and coalescing into stable right-running waves. Notably, the right-running waves in the lean case tend to be stronger and transition to detonations within a shorter distance from the closed end. This observation is consistent with the measurements in the companion experimental cases. The strut locations, marked for reference in Fig. 3, refer to the gaps in the oxidizer slot shown in Fig. 1.

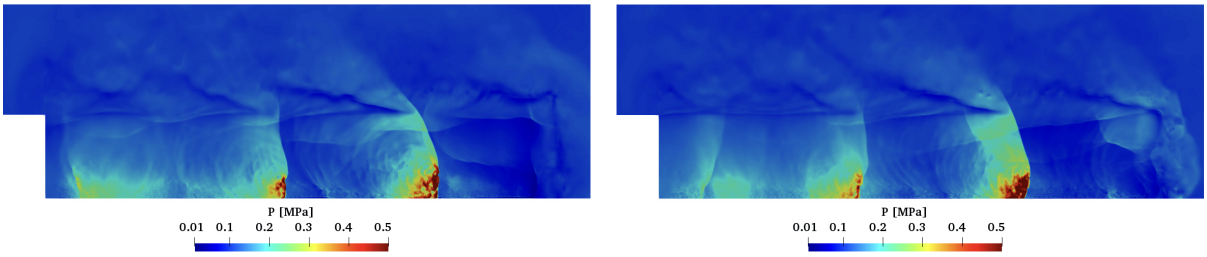

(a) Case 176 ($\phi = 0.8$). (b) Case 182 ($\phi = 1.15$).

Figure 2: Simulated pressure fields along mid-plane of oxidizer manifold and combustion chamber.

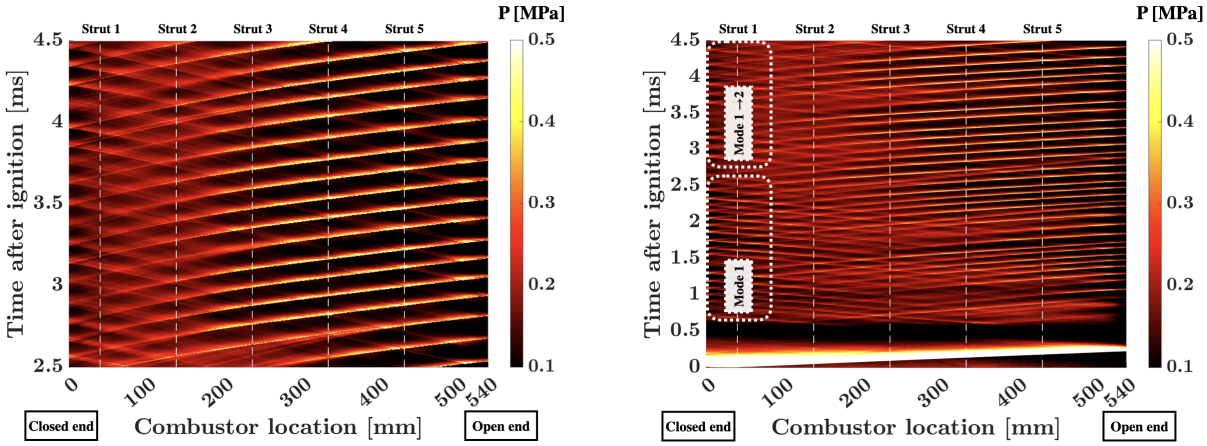

(a) Case 176 ($\phi = 0.8$). (b) Case 182 ($\phi = 1.15$).

Figure 3: Detonation surfaces from simulations, showing left- and right-running wave paths.

The additional available data for the rich case, shown in Fig. 3b, helps to identify two distinct modes which emerge in the progression towards steady-state. For about 0.25 ms after the initial detonation wave exits, the chamber remains largely quiescent with minimal pressure fluctuations while fresh reactants are resupplied from the manifolds. Then, for around 2 ms, counter-propagating waves collide and disperse near the center of the chamber, and weak left-running reacting waves transition to weak right-running detonation waves after reflecting off of the closed end. This is hypothesized to be due to a lack of fresh reactant mixture in the chamber, which is required for the waves to intensify. As time progresses, the system transitions to its second mode, characterized by minimally-reacting left-running shocks which transition to a strong right-running detonation waves after reflecting at the closed end. In this mode, collisions diffuse the incoming waves near the closed end, and the increased strength and velocity of the right-running waves become more evident as they travel towards the open end. This wave acceleration is depicted in Fig. 4, where data was collected from 2.5 ms after ignition—i.e., during mode 2 operation. Here, the simulation and experimental data are time-averaged for 2 ms and 200 ms, respec-

tively. The simulated wave speeds are calculated by tracking pressure gradient peaks 1 cm from the bottom of the chamber. The experimental wave speeds are calculated by filtering and differentiating the chemiluminescence intensity from high-speed broadband chemiluminescence imaging of the chamber.

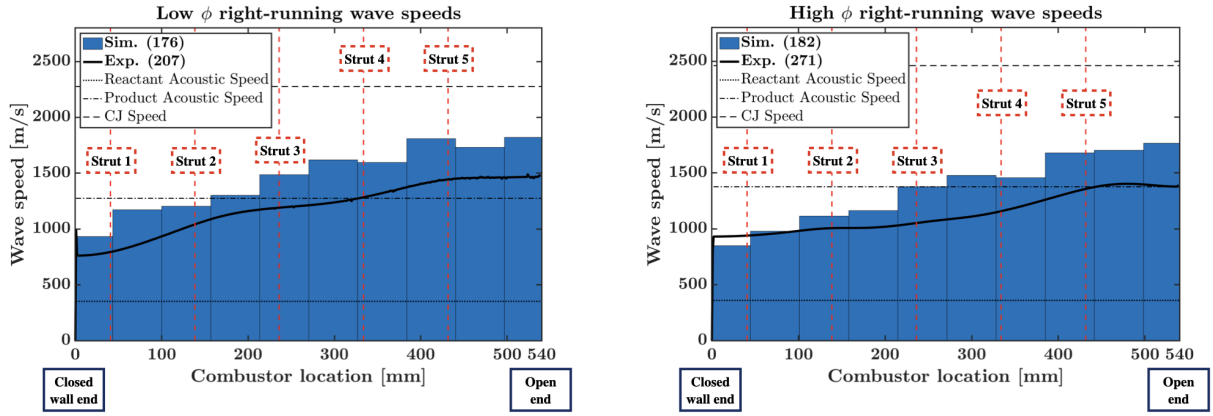

Figure 4: Time-averaged right-running wave speed comparisons between simulations and experiments. Acoustic and CJ speeds are computed with respect to ideal detonation using simulation conditions.

As noted from Fig. 3, the higher simulated wave speeds and peak pressures near the closed end of the chamber indicate that transition to strong detonation occurs after a shorter distance in the lean case. Similar trends with respect to inflow equivalence ratio were observed in the experiments. The maximum simulated wave speeds were lower than the CJ speeds by about 26% in the lean case and 33% in the rich case. This discrepancy has been noted in other studies of non-premixed detonation combustors, where incomplete mixing [3] and interactions with counter-propagating waves [8] have led to slower detonation wave speeds. The cause for the differences in wave speeds between the simulations and experiments has not yet been identified. Possible sources of discrepancy include the wave tracking methodologies, the differences in operating conditions, and the duration of available data from the simulations.

4 Conclusions

A rectangular reflective shuttling detonation combustor (RSDC) with an open-closed chamber configuration was studied to provide insight into the progression toward self-excited steady-state detonation wave behavior. The simulation results show the emergence of consistent wave patterns via two unique operating modes. The first mode consists of more numerous bi-directional weaker detonations which tend to diffuse as they collide near the center of the chamber. In this mode, the directional preference of the waves is less pronounced. This mode gradually transitions to the second mode, during which minimally-reacting waves reflect off of the closed end of the chamber and transition to strong, accelerating detonation waves supported by available reactant gases. In this mode, the diffusive wave collisions occur closer to the closed end of the chamber, and the right-running waves dominate. The low equivalence ratio case exhibited faster peak wave speeds, higher peak pressures, and shorter distances to strong detonation transition—trends also observed in the experiments. The peak wave speeds were lower than the CJ speeds for both cases, likely due to insufficient reactant mixing and counter-propagating wave interactions. Further investigations with different flow configurations may yield some insight into the observed phenomena and operating modes. For instance, preliminary studies using a closed-closed chamber configuration have exhibited a dual-mode wave behavior where the directional preference of the strong waves oscillates at regular intervals. Comparisons between closed-open and closed-closed chamber configurations can help to elucidate the effects of different wave reflection types, while pre-

mixed inflows can be studied to determine the impacts of reactant mixing. The insight into the dynamics of simplified combustors may facilitate further understanding and realization of practical RDEs.

References

[1] Kailasanath, K. (2000). Review of Propulsion Applications of Detonation Waves. AIAA Journal. 38(9): 1698.

[2] Prakash S, et al. (2020). Analysis of the detonation wave structure in a linearized rotating detonation engine. AIAA Journal. 58(12): 5063.

[3] Burr JR, Yu K. (2017). Detonation wave propagation in cross-flow of discretely spaced reactant jets. 53rd AIAA/SAE/ASEE Joint Propulsion Conference 2017: 4908.

[4] Prakash S, et al. (2021). Numerical simulation of a methane-oxygen rotating detonation rocket engine. Proc. Combust. Inst. 38(3): 3777.

[5] Chacon F, Gamba M. (2019). Detonation wave dynamics in a rotating detonation engine. AIAA Scitech 2019 Forum: 198.

[6] Bluemner R, et al. (2021). Stabilization mechanisms of longitudinal pulsations in rotating detonation combustors. Proc. Combust. Inst. 38(3): 3797.

[7] Yamaguchi M, et al. (2019). Supersonic combustion induced by reflective shuttling shock wave in fan-shaped two-dimensional combustor. Proc. Combust. Inst. 37(3): 3741.

[8] Yamaguchi M, et al. (2021). Investigation of combustion modes and pressure of reflective shuttling detonation combustor. Proc. Combust. Inst. 38(3):3615.

[9] Taguchi T, et al. (2022). Investigation of reflective shuttling detonation cycle by schlieren and chemiluminescence photography. Combust. Flame. 236: 111826.

[10] Schwinn K, et al. (2018). Self-sustained, high-frequency detonation wave generation in a semi-bounded channel. Combust. Flame. 193: 384.

[11] Greenshields CJ, et al. (2010). Implementation of semi-discrete, non-staggered central schemes in a colocated, polyhedral, finite volume framework, for high-speed viscous flows. Int J Numer Methods Fluids. 63(1): 1.

[12] Xu R, Wang H. (2018). A reduced reaction model of methane combustion. Personal comm.

[13] Smith G, Tao Y, Wang H. (2016). Foundational fuel chemistry model version 1.0 (ffcm-1). http://nanoenergy.stanford.edu/ffcm1.

[14] Barwey S, Raman V. (2021). A neural network inspired formulation of chemical kinetics. Energies. 14(9): 2710.

[15] Sato T, et al. (2021). Mixing and detonation structure in a rotating detonation engine with an axial air inlet. Proc. Combust. Inst. 38(3): 3769.

[16] Schwer D, Kailasanath K. (2012). Feedback into mixture plenums in rotating detonation engines. 50th AIAA aerospace sciences meeting: 617.

[17] Sato T, Raman V. Effects of injection pressure on performance of non-premixed rotating detonation engines. (Submitted, 2022).